Drawing of Microshear Deformation Zones in Glassy Polymers: Poly(phenylene oxide) (PPO)

A. C.-M. YANG,[1,]* R. C. WANG,[1] M. S. KUNZ,[2] and I. C. YANG[3]

[1]Department of Materials Science and Engineering, National Tsing Hua University, Hsinchu, Taiwan, R.O.C.; [2]Ciba-Geigy Corp., Switzerland; [3]Department of Electronics, National Chiao Tung University, Hsinchu, Taiwan, R.O.C.

SYNOPSIS

The topography of the microscopic shear deformation zones (SDZ) in the glassy polymer PPO was studied by using atomic force microscopy (AFM) and was used to analyze the growth and breakdown of the SDZ. It was found that the local stress and strain are almost constant within the deformation zones but higher than those in the elastic regions. The maximum strain rate during stretching was found to always locate near the SDZ boundaries, indicating that most drawing took place there. With both the local stress and strain obtained for every point within the SDZ, it is possible to construct a full stress–strain curve for the drawing of the tiny local deformation zones. The stress–strain curve clearly demonstrates a yield point in the beginning of microyielding where the tensile modulus was found to be much lower than that in the elastic regime. Some strain hardening, however, took place at larger deformation. Moreover, we found that for each microscopic region participated in the microdrawing the local strain rate increased with local strain until a critical strain around 0.65 was reached, after which the strain rate decreased with strain. This critical strain may be related to the chain entanglement network structure because it shifted to 0.75 when PS diluents were blended into PPO, indicating that strain hardening was delayed by the increase of chain entanglement mesh size.

Keywords: atomic force microscope • shear deformation zone • strain localization • strain hardening

INTRODUCTION

Prior to crack propagation, glassy polymers develop ductile or brittle mode of microdeformations, i.e., crazing and microshear yielding, respectively, or the combination of these two to release mechanical energy in response to the applied forces. The microdeformation zones, crazes, and shear deformation zones (SDZs) resulted from these mechanisms are known to have distinct mechanical stability and microstructure. The molecular processes behind the microdeformations, however, remain mysterious. In a previous study,[1] it was shown that important factors such as chemical structure, deformation temperature, and strain rate could strongly influence the microfracture behavior of polymers. Significant progress has been gained for understanding the polymer crazing process.[2] However, probably owing to the complicated morphology and the lack of contrast under a transmission electron microscopy (TEM), the SDZs in the ductile polymers were infrequently studied. Nevertheless, Kramer and his coworkers,[3,4] using the Dugdale theories,[5] successfully obtained the stress distribution along the length of the SDZ in polycarbonates. The detailed stress distributions within the SDZ that can give important information regarding the growth and breakdown of the SDZ, however, remain unexplored. Recently, we used atomic force microscopy (AFM) to study crazes in polystyrenes and found that the growth of a craze followed a micronecking process.[6] It is thus very interesting to use the same approach to study the SDZ in PPO to reveal the micromechanics of shear yielding in ductile polymers. We found that, as reported

---

* To whom correspondence should be addressed.

Journal of Polymer Science: Part B: Polymer Physics, Vol. 34, 1141–1145 (1996)
CCC 0887-6266/96/061141-05

in this article, by combining the AFM data with the appropriate plasticity theories of Bridgman[7] and Hutchinson and Neale,[8] the vital information of local stress, local strain, local tensile modulus, strain rate distribution, and stress–strain curve of the zone drawing of the SDZs could be obtained. The implications of these results are also discussed.

EXPERIMENTAL PROCEDURES

Uniform thin film poly(2,6-dimethyl-1,4-phenylene oxide) (PPO) of 0.5 μm thickness was cast from the clear toluene solution that was heated to around 70°C. The polymer was purchased from the Aldrich Chemical Company with a molecular weight of $M_w = 244{,}000$ and $M_n = 32{,}000$. After the solvent had escaped, the PPO thin film was floated off the substrate onto water surface, and picked up on a supporting copper grid that had been annealed and coated with PS to ensure good extendibility and strong adhesion to the polymer film.[9]

When the specimen preparation was complete, the specimen was stretched in a hand-operated strain jig to grow SDZs in film during which process a polarized light microscope (Zeiss Axioplan) was used to monitor the nucleation and growth of the SDZs. To obtain the detail topographic information of the deformation zones, an contact mode AFM (Nanoscope II, Digital Instruments, Inc.) was used to map out the SDZ's surface structure with a minimum contact force. Complementary to AFM, a TEM (Joel 200 FX) was used to acquire the through-thickness high resolution images and line scan mass distribution of SDZs. Combining the data from AFM surface profile and the TEM mass distribution, it is possible to produce the relative density distribution across the tiny SDZs. Finally, the AFM topographical data of the SDZ were input into a personal computer for calculation to generate the important micromechanical data.

RESULTS AND DISCUSSIONS

SDZ Growth by Micronecking

For a typical SDZ in the PPO film, the surface profile obtained from AFM always demonstrates a large depression in the deformation region, as shown in Figure 1a. The maximum depth in the depression was found to increase linearly with the zone width, eventually reaching a saturated value at a critical width around 5 μm, as shown in Figure 1b. This behavior indicates that the growth of SDZs, similar to that of crazes, also follows a micronecking process.

The relative mass density within the SDZ, defined as the local mass density normalized to that of the undeformed PPO, could be obtained from the TEM line scan data that gives the mass distribution, corrected by the AFM surface profile. Following Lauterwasser and Kramer,[9] the mass fraction M_f inside the microdeformation zone could be expressed as $M_f = 1 - \ln[\varphi_d/\varphi_f]/\ln[\varphi_h/\varphi_f]$, where φ_d, φ_f, and φ_h are, respectively, the optical densities in the TEM negative of the regions inside and outside the SDZ, and that of a through hole. The distribution of the relative mass density was obtained by dividing the mass fraction M_f by the local thickness within the SDZ obtained from AFM. It was found that the relative mass density, within or outside the SDZ, is approximately constant to be around 1. This indicates that the mass density does not change during the course of microshear yielding in the PPO films.

Analysis of Stress Distribution in the SDZ

Because the growth of SDZ follows a micronecking process and the mass density remains constant throughout the drawing process, the Bridgman's necking theory[7] is used to analyze the stress distribution within the SDZ from the AFM topographic data. In this analysis, the lateral contraction in the width direction was ignore because the thin film under stretching was firmly bonded to the copper grid to restrict any significant lateral contraction. Following Bridgman, the tensile and shear stresses inside the necked region could be expressed, respectively, as

$$\sigma_t = F \cdot tw\beta/2 \qquad (1)$$

$$\sigma_s = \sigma_t/2\cos^2\alpha \qquad (2)$$

for a neck with a radius of curvature R and a thickness of 2τ, where β is a correction factor given as

$$\beta = \{(1 + 2R/\tau)^{1/2} \cdot \log[1 + \tau/R + (2\tau/R)^{1/2} \cdot (1 + \tau/2R)^{1/2}] - 1\}^{-1}, \qquad (3)$$

in that F is the load, w is the width of the film, and α is the surface tangent at any point in the necked region.

The tensile stress σ_t obtained for a SDZ with a width of approximately 5 μm is plotted in Figure 2a. The stress σ_t is almost constant within the SDZ but

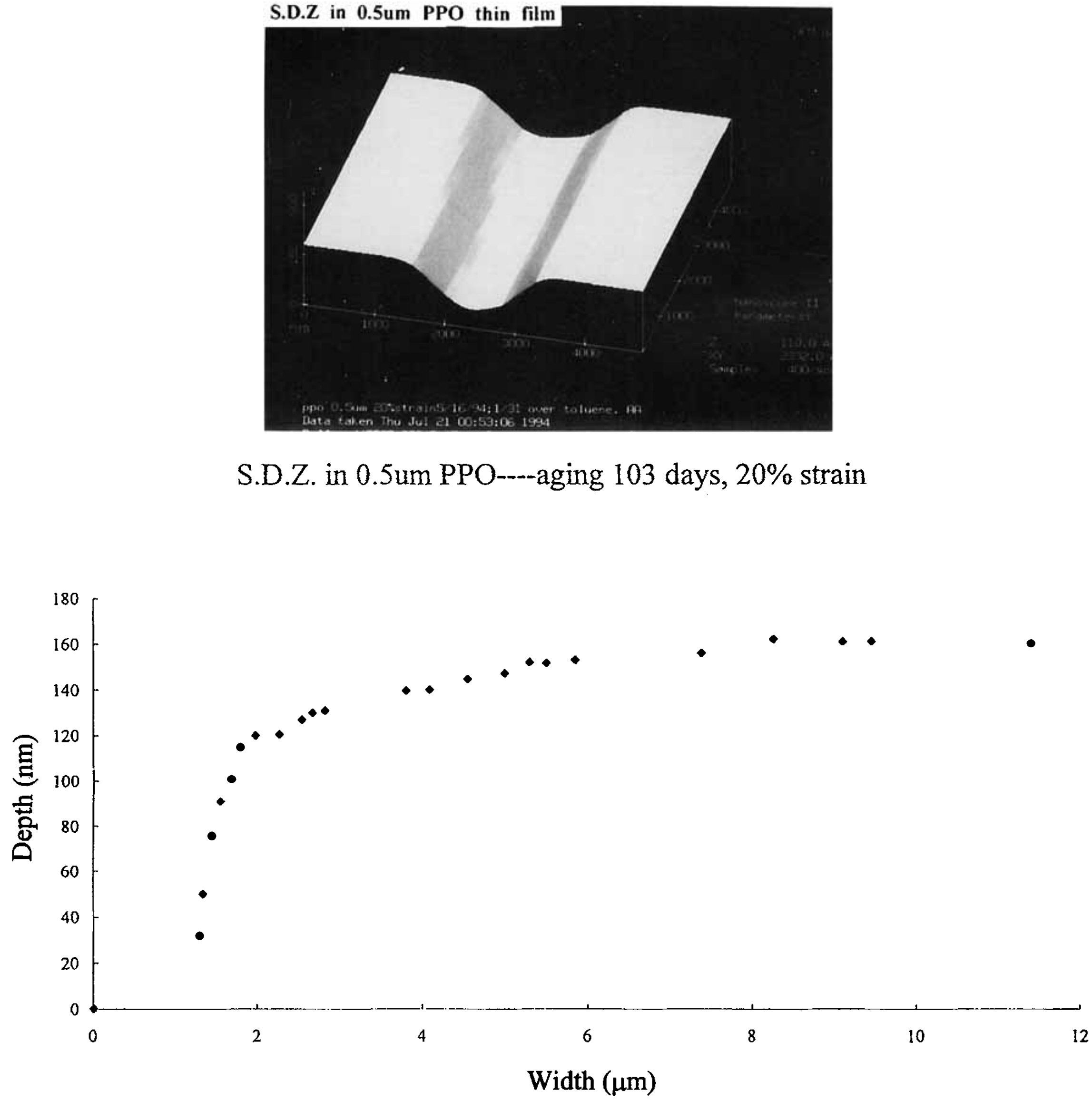

S.D.Z. in 0.5um PPO----aging 103 days, 20% strain

Figure 1. (a) A typical AFM topographic data of a SDZ in PPO films, and (b) the depression versus the width of the SDZ in PPO films.

of a magnitude more than double of those outside the zone. Apparently, the stress concentration at the neck is due to the decrease in cross-sectional area of the SDZ regions. The shear stress σ_s behaves similarly to the tensile stress but is of approximately one-half the tensile value.

Strain Information and the Stress–Strain Curve of SDZ Microdrawing

The strain and the instantaneous strain rate at any point inside the neck could also be determined from the AFM topographic data by following the analysis of Hutchinson and Neale.[8] For a neck with a thicknesses distribution of $\tau(x)$ and widening speed of V_p, the strain $\varepsilon(x)$ and strain rate $\dot{\varepsilon}(x)$ in a SDZ could be expressed as:

$$\varepsilon(x) = \ln[\tau_0/\tau(x)] \tag{4}$$

$$\dot{\varepsilon}(x) = -V_p \cdot \{\exp[\varepsilon(x) - \varepsilon_0]/\tau(x)\} \times [\partial\tau(x)/\partial x] \tag{5}$$

where "0" denotes the region outside the neck. For simplicity, V_p is assumed to be constant during the growth of a SDZ.

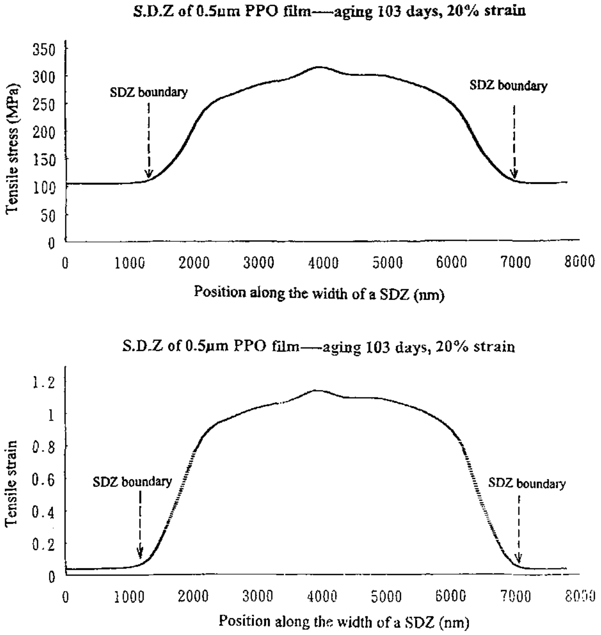

Figure 2. (a) The tensile stress across the width of a SDZ, and (b) the strain distribution across the width of a SDZ.

Figure 2b shows the strain distribution across the width of a SDZ that is the drawing direction. The strain inside the SDZs, approximately 100%, is much higher than that outside the SDZ, which maintained an approximately constant strain at 3.5%, the nucleation strain of the SDZ, because the SDZ act as the deformation sink for the external deformation. The strain in the SDZ is roughly constant but decreases towards the boundary regions. This result, calculated from AFM topography data, is in excellent agreement with the TEM microdensitometry data obtained by Kramer that the draw ratio of the SDZ is around 2.[4]

When the local stress is cross-plotted with the local strain for the data taken across the zone width from the bulk to the SDZ center, a true stress versus true strain curve was obtained for the drawing of the microscopic SDZ in the PPO thin films. Such a result is shown in Figure 3. The stress–strain curve clearly demonstrates a prominent yield point at the onset of strain localization at the beginning of micronecking. After yielding, the effective modulus decreased by approximately an order of magnitude compared to that in the bulk. This result is in good agreement with that obtained in a separated experiment using an AFM deflection technique[10] on PPO thin films. As shown in the stress–strain curve, the modulus increased slightly as the strain increased, indicating that some strain hardening took place later, however.

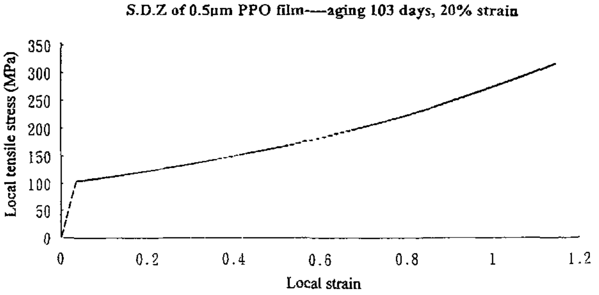

Figure 3. The local stress versus local strain during the drawing of a SDZ.

The strain rate distribution normalized to a constant V_p along the SDZ width obtained from eq. (5) exhibits a large maximum at each of the boundary regions, indicating that most drawing took place there during the widening of SDZs. Once drawn into the central region in a SDZ, however, the polymer deformation becomes much slower, consistent with the observed strain hardening in Figure 3. This result agrees qualitatively with a surface drawing mechanism for zone widening but the breadth of the "active zones" should be in the order of 0.1–0.2 μm.

It is interesting to note that when the local strain rate was plotted against the local strain, the strain rate was found to increase with strain up to a critical strain $\varepsilon_{\max}$ where the strain rate reaches a maximum and thereafter decreases with increasing strain. The curve is shown in Figure 4. The critical strain $\varepsilon_{\max}$ corresponding to the maximum strain rate is approximately 0.65 for PPO thin films deformed at the ambient conditions. The curve of strain rate versus strain, however, shifted to higher strain in that the critical strain $\varepsilon_{\max}$ increased to 0.75 when a 20% weight fraction of low molecular weight polystyrene (M_w = 2,000) was blended into PPO. The low molecular weight diluent of PS molecules, which

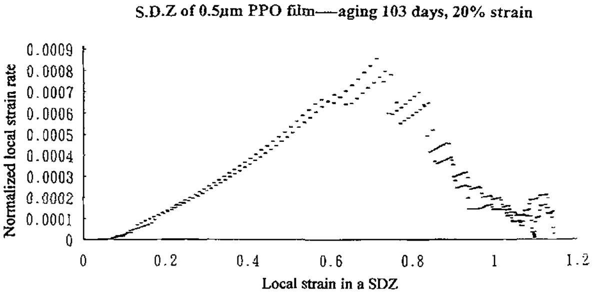

Figure 4. The normalized local strain rate versus local strain in a SDZ.

are miscible with the PPO, apparently had delayed the strain hardening during the microdeformation process, possibly due to the decrease of the entanglement density, or equivalently the increase of contour length of PPO chain between adjacent entanglements.

CONCLUSIONS

It can be concluded that the growth of the SDZ in PPO films follows a micronecking mechanics. The local density of the polymer remain unchanged before and after the drawing of the SDZ. Both strain and stress concentrated inside the SDZ and stayed almost constant within the zone. The strain rate has the maximum value at the boundary regions, indicating that most drawing took place there during zone widening. The stress–strain curve indicates a significant strain softening taking place after the onset of microdrawing. However, some strain hardening was observed once the polymer was drawn into the SDZ.

The research was sponsored by the National Science Council of R.O.C., Taiwan (NSC 84-2216-E-007-020) and supported by a joint research study with Dr. Do Yoon at the IBM Almaden Research Center at San Jose, CA, USA.

REFERENCES AND NOTES

1. S. T. Wellinghoff and E. B. Baer, *J. Appl. Polym. Sci.*, **22,** 2025 (1978).
2. E. J. Kramer, *Adv. Polym. Sci.*, **52/53,** 1 (1983).
3. A. M. Donald and E. J. Kramer, *J. Mater. Sci.*, **16,** 2977 (1981).
4. A. M. Donald and E. J. Kramer, *Polymer*, **23,** 461 (1982).
5. D. S. Dugdale, *J. Mech. Sol.*, **8,** 100 (1960).
6. A. C.-M. Yang, M. S. Kunz, and J. A. Logan, *Macromolecules*, **26,** 1767 (1993).
7. P. W. Bridgman, *Studies in Large Plastic Flow and Fracture*, Harvard University Press, Cambridge, MA, 1964, p. 9.
8. J. W. Hutchinson and K. W. Neale, *J. Mech. Phys. Solid*, **31,** 405 (1983).
9. B. D. Lauterwasser, Ph.D. thesis, Cornell University, 1979, p. 111.
10. A. C.-M. Yang, *Mater. Chem. Phys.*, **41**(4), 295 (1995).

Received March 20, 1995
Revised October 23, 1995
Accepted November 2, 1995